

# A comparison on spray absorption performance of $\text{LiNO}_3\text{-NH}_3$ and $\text{H}_2\text{O-NH}_3$ systems

M. Venegas<sup>1</sup>, M. Izquierdo<sup>2</sup>, P. Rodríguez<sup>3</sup>, A. Lecuona<sup>3</sup>

1. Departamento de Ingeniería Térmica y de Fluidos, Universidad Carlos III de Madrid  
Avda. Universidad 30, 28911 Leganés, Madrid, Spain

2. Instituto de Ciencias de la Construcción Eduardo Torroja (CSIC), C. Serrano Galvache,  
s/n, 28033, Madrid, Spain. E-mail: [mizquierdo@ietcc.csic.es](mailto:mizquierdo@ietcc.csic.es)

3. Unidad Asociada de Ingeniería Térmica y de Fluidos UC3M-CSIC, Universidad Carlos  
III de Madrid Avda. Universidad 30, 28911 Leganés, Madrid, Spain

In the present work the spray absorption method is studied for the absorption of ammonia refrigerant vapour by lithium nitrate – ammonia, and water – ammonia solutions. Mass transfer coefficients attainable using the spray absorption method in the low-pressure absorber of a double-stage absorption refrigeration system are calculated. The results show that the mass transferred is maximum (about 60 % of the total) during the droplets deceleration period for the lithium nitrate – ammonia solution. This period represents about 12.5 % of the droplets residence time inside the absorber until they reach the equilibrium state. An average mass transfer coefficient equal to  $k_m = 18.6 \cdot 10^{-5}$  m/s may be attained. In the case of the water – ammonia solution, during the droplets deceleration period about 99 % of the ammonia vapour is absorbed. This period represents almost 100 % of the droplets residence time inside the absorber. An average mass transfer coefficient equal to  $k_m = 11 \cdot 10^{-4}$  m/s may be obtained.

## 1. Introduction

Traditionally laminar falling film absorbers are used in absorption refrigeration systems. However, at present other absorption methods are being studied aiming the reduction of the heat and mass transfer area and consequently of the absorber dimensions. This reduction could be performed increasing the contact surface between the solution and the refrigerant vapour. One method for maximising the interfacial area, known as spray absorption, consists on dispersing the solution in small droplets inside an adiabatic chamber. The absorption heat is extracted using a conventional plate heat exchanger.

If spray absorption is used the mass and heat transfer processes are divided in separate apparatus and the absorption occurs inside the adiabatic chamber. In this case the heat transfer coefficients increase considerably because the heat exchange equipment to use is a conventional liquid – liquid exchanger. The resulting area can be about one half that of a conventional falling film absorber. If we take into account the no complexity and the low price of the absorption chamber, then the total costs of the machine can be significantly reduced.

Some theoretical and experimental studies about droplets absorption using water as refrigerant have been developed [1-8]. Nevertheless, as far as we know, there are no reported studies on spray absorption systems employing ammonia as refrigerant. In this paper we study the lithium nitrate – ammonia ( $\text{LiNO}_3\text{-NH}_3$ ) and water – ammonia ( $\text{H}_2\text{O-NH}_3$ ) systems.

The objective of this paper is to determine and compare the mass transfer coefficient attainable using the spray absorption method and the  $\text{LiNO}_3\text{-NH}_3$  and  $\text{H}_2\text{O-NH}_3$  solutions.

Numerical computations are used to solve heat and mass transfer conservation equations. In a previous paper, Venegas et al. [9] presented results for the droplets deceleration period inside the absorption chamber using the  $\text{LiNO}_3\text{-NH}_3$  solution.

## 2. Analysis

For this study the  $\text{LiNO}_3\text{-NH}_3$  and  $\text{H}_2\text{O-NH}_3$  solutions and ammonia vapour properties have been taken from Infante Ferreira [10,11], Kusaka et al. [12], IAR [13] and ASHRAE [14]. In Table 1 and Table 2 the subcooled solutions and vapour properties are shown respectively. These data correspond to the conditions of the low-pressure absorber of the double-stage refrigeration machine analysed by Izquierdo et al. [15] and Venegas et al. [16].

Calculation of the mass transfer coefficients is performed considering the atomiser zones shown in Figure 1: intact length, droplet deceleration and uniform movement.

**Table 1a.**  $\text{LiNO}_3\text{-NH}_3$  solution properties.

$x$ (%)	$T$ (°C)	$P$ (bar)	$\rho_d$ (kg/m <sup>3</sup> )	$\mu_d$ (mPa·s)	$C_p$ (kJ/kg K)	$R$ (μm)	$\sigma$ (N/m)	$\alpha$ (m <sup>2</sup> /s)	$D$ (m <sup>2</sup> /s)	$L$ (kJ/kg)
36.7	40	2.36	1132	7.62	2.62	30	0.052	$5.1 \cdot 10^{-7}$	$0.74 \cdot 10^{-9}$	$1.31 \cdot 10^3$

**Table 1b.**  $\text{H}_2\text{O-NH}_3$  solution properties.

$x$ (%)	$T$ (°C)	$P$ (bar)	$\rho_d$ (kg/m <sup>3</sup> )	$\mu_d$ (mPa·s)	$C_p$ (kJ/kg K)	$R$ (μm)	$\sigma$ (N/m)	$\alpha$ (m <sup>2</sup> /s)	$D$ (m <sup>2</sup> /s)	$L$ (kJ/kg)
31.2	40	2.39	863.4	0.485	4.42	30	0.054	$1.5 \cdot 10^{-7}$	$1.77 \cdot 10^{-9}$	$1.31 \cdot 10^3$

**Table 2.** Ammonia vapour properties.

$T_{sh}$ (°C)	$T_s$ (°C)	$\rho_c$ (kg/m <sup>3</sup> )	$\mu_c$ (Pa s)
10	-15	1.76	$9.8 \cdot 10^{-6}$

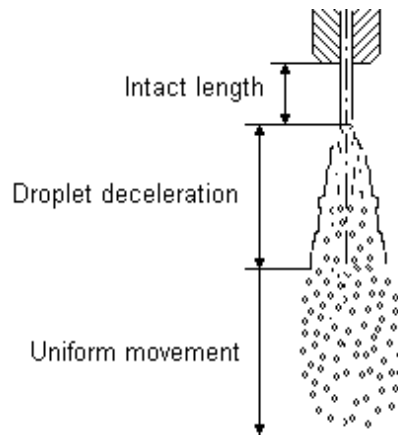


**Fig. 1** Atomisation process zones.

### 2.1. Intact Length

For the estimation of the mass transfer coefficients in this zone the relation given by Ryan et al. [5], Equation (1), valid for Graetz ( $Gr$ ) numbers greater than 100, is used.

$$k_m = \left( \frac{uD}{2L_c\pi} \right)^{0.5} \quad (1)$$

The lengths of the intact zones are calculated using the relation proposed by Bayvel and Orzechowski [17]:

$$L_c = 8.25d_0We^{0.25}Lp^{-0.4} \left( \frac{\rho_c}{\rho_d} \right)^{-0.6} \quad (2)$$

## 2.2. Droplets deceleration

In this zone the simulation model described in Venegas [18] is used. A single spherical droplet of radius  $R$  translating and experimenting absorption of ammonia vapour is considered. The model bases on the following hypothesis:

- a) The droplet keeps the spherical form during its fall.
- b) The heat release occurs at the interface between the droplet and the surrounding vapour.
- c) The radius of the droplet is constant.
- d) The coalescence and collisions between droplets are not considered.
- e) The contribution to mass transfer of the liquid film falling by the absorber wall is insignificant.

A numerical simulation procedure is used for determining the mass transfer coefficient achievable during the spray absorption of ammonia vapour by solution droplets. This procedure is based on the simultaneous solution of the heat and mass transfer conservation equations in a solution droplet, together with the appropriate initial and boundary conditions:

$$\frac{\partial x}{\partial t} + u_r \cdot \frac{\partial x}{\partial r} + \frac{u_\theta}{r} \frac{\partial x}{\partial \theta} = D \left( \frac{\partial^2 x}{\partial r^2} + \frac{2}{r} \frac{\partial x}{\partial r} + \frac{\cot \theta}{r^2} \frac{\partial x}{\partial \theta} + \frac{1}{r^2} \frac{\partial^2 x}{\partial \theta^2} \right) \quad (3)$$

$$\frac{\partial T}{\partial t} + u_r \cdot \frac{\partial T}{\partial r} + \frac{u_\theta}{r} \frac{\partial T}{\partial \theta} = \alpha \left( \frac{\partial^2 T}{\partial r^2} + \frac{2}{r} \frac{\partial T}{\partial r} + \frac{\cot \theta}{r^2} \frac{\partial T}{\partial \theta} + \frac{1}{r^2} \frac{\partial^2 T}{\partial \theta^2} \right) \quad (4)$$

The initial conditions are:

$$\text{for } t = 0, x = x_o \text{ and } T = T_o \text{ for all } r \quad (5)$$

The boundary conditions are:

$$\text{in } r = 0, \frac{\partial x}{\partial r} = \frac{\partial T}{\partial r} = 0 \text{ for } t > 0 \quad (6)$$

$$\text{in } r = R, x = x_{eq} \text{ and } T = T_{eq} \text{ for } t > 0 \quad (7)$$

Also in  $r = R$ :

$$x_{eq} = a \cdot T_{eq} + s \quad (8)$$

$$q = -L \cdot m \quad (9)$$

$$\text{in } \theta = 0 \text{ and } \theta = \pi, \frac{\partial x}{\partial \theta} = \frac{\partial T}{\partial \theta} = 0 \text{ for } t > 0 \quad (10)$$

Velocity components inside droplets should be known before solving the system of Eqs. (3)-(10). Equations to use for the radial and angular velocities depend on the droplets Reynolds

number. For  $Re < 1$  the radial and angular velocity components are obtained using the Hadamard – Rybczynski equations. In the case of  $10 \leq Re \leq 250$  the equations reported by Uribe-Ramírez and Korchinsky [19] are used. In the present study the droplets Reynolds number varies from high  $Re$  at the atomiser outlet, because of the high initial velocity, to  $Re$  between 1 and 10 for the droplets terminal velocity. In the case of Reynolds numbers in the range  $1 \leq Re < 10$ , the results obtained using the Hadamard – Rybczynski equations should be approximately valid. This is because, according to Clift et al. [20], the fluid recirculation and wake formation in the rear of the droplet only begin for Reynolds numbers higher than 20. For the numerical solution of Eqs. (3) and (4) and the corresponding initial and boundary conditions (5)-(10) the finite difference method is used. The application of the finite difference technique to partial differential equations, as Eq. (3) and (4), is described by Anderson et al. [21]. This technique has been extensively used [22,23] to solve heat or mass transfer problems in spherical droplets. A totally implicit method has been selected, in this case the Crank-Nicholson method [24,25].

### 2.3. Uniform movement

In this zone the calculation of the mass transfer coefficients is also made using the simulation procedure. Droplets have already achieved their terminal velocity and the initial conditions for the simulation correspond to the final conditions of the droplets deceleration process.

## 3. Mass transfer coefficients

### 3.1. Intact length

In the present case  $Gr = 3.1 \cdot 10^4$  for the  $LiNO_3-NH_3$  pair and  $Gr = 1.5 \cdot 10^5$  for the  $H_2O-NH_3$  solution. Then, Eq. (1) can be applied. The mass transfer coefficients obtained are  $k_m = 1.98 \cdot 10^{-4}$  m/s for the  $LiNO_3-NH_3$  solution and  $k_m = 10.3 \cdot 10^{-4}$  m/s for the  $H_2O-NH_3$  pair.

These mass transfer coefficients are very high. However, the interfacial area is lower than the one obtained after the fragmentation of the liquid columns. Also the residence time of the fluid particles in this zone is very short because of the high initial velocity of the fluid. For these reasons the mass transferred in this zone is not high, as later will be shown.

### 3.2. Droplets deceleration

From the simultaneous solution of Eqs. (3)-(10) the variation of ammonia concentration and temperature in the  $LiNO_3-NH_3$  and  $H_2O-NH_3$  solution droplets is obtained. Figure 2 shows the increase of ammonia concentration, as a function of time, during the period of droplet deceleration inside the absorption chamber for the  $LiNO_3-NH_3$  solution. This period corresponds to 0.081 seconds for the given conditions.

Figure 2 shows that at the beginning of the deceleration period the area near to the droplet surface ( $r = R$ ) achieves a high concentration of ammonia. This concentration increase is less pronounced in the medium zone ( $r = R/2$ ) and the droplet central point ( $r = 0$ ) keeps at the initial concentration (36.7 %). Gradually ammonia is diffused from the surface to the droplet centre. At the end of the deceleration period the ammonia concentration at the droplet central point has already increased to 37 % and the average ammonia concentration of the droplet is equal to 37.9 %. This value is achieved in 0.081 seconds and it corresponds to 63 % approach to equilibrium. As it can be seen the ammonia concentration increases very rapidly in the

droplet. This is because the droplet diameter is small. The average mass transfer coefficient obtained in this zone is  $k_m = 8.6 \cdot 10^{-4}$  m/s.

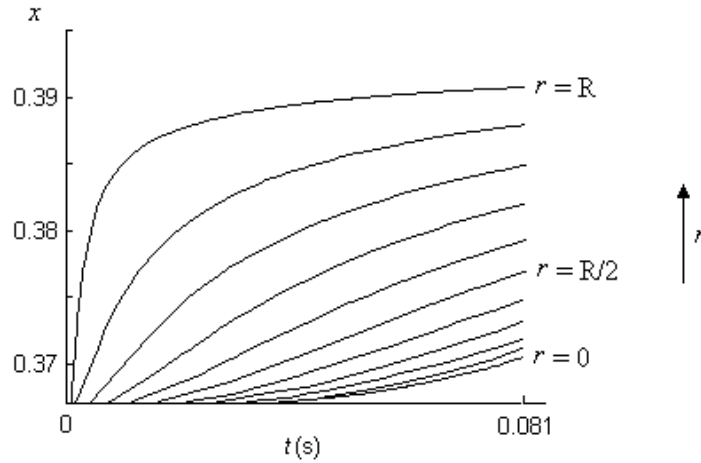


**Fig. 2** Increase of ammonia concentration on time for the  $\text{LiNO}_3\text{-NH}_3$  solution.

Figure 3 shows the evolution of ammonia concentration in the droplet during the deceleration period for the  $\text{H}_2\text{O-NH}_3$  system. It can be seen a more rapid increase of ammonia concentration than in the  $\text{LiNO}_3\text{-NH}_3$  system. In the case of the  $\text{H}_2\text{O-NH}_3$  solution the equilibrium state is reached in 0.0445 seconds, when the droplets are still moving in the deceleration region. That is, droplets achieve the equilibrium state before they reach their terminal velocity. Consequently, the length required for the absorption chamber will be smaller than that required for the  $\text{LiNO}_3\text{-NH}_3$  system. Average mass transfer coefficient obtained in this zone for the  $\text{H}_2\text{O-NH}_3$  solution is  $k_m = 11.1 \cdot 10^{-4}$  m/s.

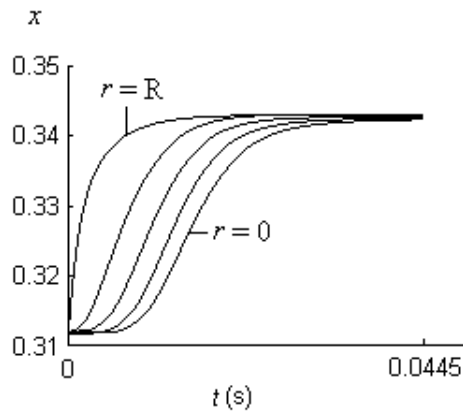


**Fig. 3** Increase of ammonia concentration on time for the  $\text{H}_2\text{O-NH}_3$  solution.

### 3.3. Uniform movement

In the uniform movement zone the  $\text{LiNO}_3\text{-NH}_3$  droplets achieve the equilibrium state. The calculation of the mass transfer coefficient was also performed using the simulation procedure. The mass transfer coefficient obtained is  $k_m = 0.81 \cdot 10^{-4}$  m/s. The time required to achieve the equilibrium during the droplets movement at constant velocity is 0.52 seconds.

## 4. Absorption results

### 4.1. $\text{LiNO}_3\text{-NH}_3$ solution

Table 3 summarises the results obtained in the present study for the low-pressure absorber of the double-stage  $\text{LiNO}_3\text{-NH}_3$  absorption system considered. As it can be seen the uniform movement zone determines the residence time of droplets inside the absorber. This zone represents an average value equal to 86.1 % of the total time required to achieve the equilibrium state.

The mass transferred in each spray zone is a function of the mass transfer coefficient, the interfacial area and the time of contact between solution and vapour. This relation can be expressed through the dimensionless parameter  $\Gamma$  defined as:

$$\Gamma = k_m \cdot A_{\text{int}} \cdot t \quad (11)$$

In Table 3 it can be observed that  $\Gamma$  is more than 2 orders of magnitude higher in the droplets deceleration and uniform movement zones than the value obtained in the intact length zone. That is, the mass transferred inside the absorption chamber is determined by the vapour absorption from the fragmentation of the liquid column in droplets. During the droplets deceleration period about 60 % of the total mass absorbed is transferred. This period represents about 13.4 % of the droplet residence time inside the absorber to achieve the equilibrium state.

**Table 3.**  $\text{LiNO}_3\text{-NH}_3$  mass transfer parameters in each spray zone.

Spray zone (Figure 1)	$L_{ac}$ (cm)	$t$ (s)	$t_r$ (%)	$k_m \cdot 10^4$ (m/s)	$A_{\text{int}} \cdot 10^{-4}$ (m <sup>2</sup> /m <sup>3</sup> )	$\Gamma$
Intact length	6	0.003	0.5	1.98	2.2	0.013
Droplet deceleration	12	0.081	13.4	8.60	10	6.97
Uniform movement	2.4	0.52	86.1	0.81	10	4.21

Average mass transfer coefficient inside the absorber is  $1.86 \cdot 10^{-4}$  m/s. This mass transfer coefficient is one order of magnitude higher than the experimental values obtained using the  $\text{LiBr-H}_2\text{O}$  solution and falling film absorbers (Table 5). In the case of falling film absorbers using the  $\text{NH}_3\text{-H}_2\text{O}$  solution the mass transfer coefficients reported have the same order of magnitude. Unluckily there are not available data for comparison with falling film absorbers using the  $\text{LiNO}_3\text{-NH}_3$  solution.

### 4.2. $\text{H}_2\text{O-NH}_3$ solution

Table 4 summarises similar results for the  $\text{H}_2\text{O-NH}_3$  system. In this case, droplets deceleration zone determines the residence time of droplets inside the absorber. This zone represents an average value equal to 99.4 % of the total time required to achieve the equilibrium state.

**Table 4.**  $\text{H}_2\text{O-NH}_3$  mass transfer parameters in each spray zone.

Spray zone (Figure 1)	$L_{ac}$ (cm)	$t$ (s)	$t_r$ (%)	$k_m \cdot 10^4$ (m/s)	$A_{\text{int}} \cdot 10^{-4}$ (m <sup>2</sup> /m <sup>3</sup> )	$\Gamma$
Intact length	0.6	0.00026	0.6	10.3	2.2	0.006
Droplet deceleration	6.1	0.0445	99.4	11.1	10	4.94

Table 4 shows that  $\Gamma$  is near to 3 orders of magnitude higher in the droplets deceleration region than the value obtained in the intact length zone. Here also, the mass transferred inside the absorption chamber is determined by the vapour absorption from the fragmentation of the

liquid column in droplets. During the droplets deceleration period almost 100 % of the total mass absorbed is transferred.

Average mass transfer coefficient inside the absorber is  $11 \cdot 10^{-4}$  m/s. This value is one order of magnitude higher than the experimental values obtained using the  $\text{H}_2\text{O}-\text{NH}_3$  solution and falling film absorbers (Table 5).

**Table 5.** Typical values of  $k_m$  in falling film absorbers.

Reference	Method	Solution	$k_m \cdot 10^5$
Hoffmann and Ziegler [26]	Experimental	$\text{NH}_3\text{-H}_2\text{O}$	10 – 35
Kang et al. [27]	Experimental	$\text{NH}_3\text{-H}_2\text{O}$	1 – 55
Kim et al. [28]	Experimental	$\text{LiBr-H}_2\text{O}$	0.5 – 0.7
Miller and Perez-Blanco [29]	Experimental	$\text{LiBr-H}_2\text{O}$	1.2 – 3.8

## 5. Conclusions

$\text{LiNO}_3\text{-NH}_3$  and  $\text{H}_2\text{O-NH}_3$  spray absorption systems, from the mass transfer point of view, have been theoretically investigated in the present work. Droplets absorption determines the mass transferred inside the adiabatic spray absorbers. During the droplets deceleration period about 60 % of the total mass absorbed is transferred in the case of the  $\text{LiNO}_3\text{-NH}_3$  solution and almost 100 % in the case of the  $\text{H}_2\text{O-NH}_3$  pair.

In the case of the  $\text{LiNO}_3\text{-NH}_3$  system, this period represents about 13.4 % of the droplets residence time inside the absorption chamber to achieve the equilibrium state. The droplets stay in the uniform movement zone approximately 86.1 % of the residence time. For the  $\text{H}_2\text{O-NH}_3$  solution, droplets deceleration period represents near to 100 % of the droplets residence time.

When the  $\text{H}_2\text{O-NH}_3$  spray absorption is used a high mass transfer coefficient may be obtained ( $k_m = 11 \cdot 10^{-4}$  m/s). This value is one order of magnitude higher than the value obtained in the present study for the  $\text{LiNO}_3\text{-NH}_3$  system ( $k_m = 18.6 \cdot 10^{-5}$  m/s). Also it is one order of magnitude higher than the experimental values obtained using falling film absorbers and the  $\text{H}_2\text{O-NH}_3$  solution. As could be expected the use of small droplets is recommended for spray absorption in ammonia systems because a rapid increase of ammonia concentration is achieved.

## Acknowledgements

The authors wish to express their gratitude to the Ministerio de Ciencia y Tecnología for the financial support through the projects DPI2002-02439. Also, M. Venegas wishes to thank to the Agencia Española de Cooperación Internacional for the PhD fellowship granted.

## Nomenclature

$a$	constant in equilibrium equation	$Gr$	Graetz number, $2d_{01}^2 u / DL_c$
$A_{\text{int}}$	interfacial area per unit of volume, $\text{m}^2/\text{m}^3$	$k_m$	mass transfer coefficient, m/s
$C_p$	specific heat, $\text{kJ/kg K}$	$L$	latent heat, $\text{kJ/kg}$
$D$	diffusion coefficient, $\text{m}^2/\text{s}$	$L_{ac}$	length of spray zone, cm
$d_0$	atomiser hole diameter, m	$L_c$	intact column length, m
$d_{01}$	liquid column diameter, $d_0 \sqrt{\psi}$	$Lp$	Laplace number, $\rho_d d_0 \sigma / \mu_d^2$

$m$	mass flux, kg/m <sup>2</sup> s
$P$	pressure, Pa
$q$	heat flux, kW/m <sup>2</sup>
$r$	radial distance, m
$R$	droplet radius, m
$s$	constant in equilibrium equation
$t$	time, s
$t_r$	relative time, %
$T$	temperature, K
$u$	droplets velocity, m/s
$We$	Weber number, $\rho_d d_0 u^2 / \sigma$
$x$	refrigerant mass fraction in the liquid phase, kg/kg

#### Greek symbols

$\alpha$	thermal diffusivity, m <sup>2</sup> /s
$\Gamma$	mass transfer dimensionless parameter
$\mu$	viscosity, Pa s
$\theta$	angle in spherical coordinate
$\rho$	density, kg/m <sup>3</sup>
$\sigma$	surface tension, N/m
$\psi$	contraction coefficient, dimensionless

#### Subscripts

$c$	continuous
$d$	disperse
$eq$	thermodynamic equilibrium
$o$	initial instant
$r$	radial direction
$sh$	superheated

## References

- [1] Ryan W A 1994 *AES-Vol. 31, Int. Absorption Heat Pump Conf.* 155-62
- [2] Paniev G A 1983 *Heat Transfer-Soviet Research* **15** 62-72
- [3] Burdukov A P, Dorokhov A R and Paniev G A 1989 *Soviet J. Applied Physics* **3** 39-45
- [4] Morioka I, Kiyota M, Ousaka A and Kobayashi T 1992 *JSME Int. J. Series II* **35** 458-64
- [5] Ryan W A, Ruiz F and Wurm J 1995 *Proc. Int. Gas Research Conf.* 1483-93
- [6] Summerer F, Riesch P, Ziegler F and Alefeld G 1996 *ASHRAE Technical Data Bulletin* **12** 50-7
- [7] Flamensbeck M, Summerer F, Riesch P, Ziegler F and Alefeld G 1998 *Appl. Therm. Eng.* **18** 413-25
- [8] Jeong S and Garimella S 2002 *Int. J. Heat Mass Transfer* **45** 1445-58
- [9] Venegas M, Arzoz D, Rodríguez P and Izquierdo M 2003 *Int. Comm. Heat Mass Transfer* (In press)
- [10] Infante Ferreira C A 1984 *Sol. Energy* **32** 231-6
- [11] Infante Ferreira C A 1985 Ph.D. thesis, Delft Technical University, Delft, Holland
- [12] Kusaka R, Ban K, Nakamura Y and Shimokawa S 1987 *J. Phys. Chem.* **91** 985-987
- [13] IAR 1993 *Ammonia Data Book* (Washington: Int. Institute of Ammonia Refrig.)
- [14] ASHRAE 1993 *Fundamentals Handbook* (Atlanta: ASHRAE)
- [15] Izquierdo M, Venegas M, de Vega M and Rodríguez P 2001 *Proc. 7<sup>th</sup> REHVA World Congress*
- [16] Venegas M, Izquierdo M, de Vega M and Lecuona A 2002 *Int. J. Energy Res.* **26** 775-91
- [17] Bayvel L and Orzechowski A 1993 *Liquid Atomization* (Taylor & Francis)
- [18] Venegas M 2002 Ph.D. thesis, Carlos III University of Madrid, Spain
- [19] Uribe-Ramírez A R and Korchinsky W J 2000 *Chem. Eng. Sci.* **55** 3305-18
- [20] Clift R, Grace J R and Weber M E 1978 *Bubbles, drops, and particles* (NY: Academic Press)
- [21] Anderson D A, Tannehill J C and Pletcher R H 1984 *Computational Fluid Mechanics and Heat Transfer* (Taylor & Francis)
- [22] Juncu Gh 2001 *Int. J. Heat Mass Transfer* 2239-46
- [23] Lu H H, Wu T Ch, Yang Y M and Maa J R 1998 *Int. Comm. Heat Mass Transfer* 1115-26
- [24] Merrill T and Perez-Blanco H 1997 *Int. J. Heat Mass Transfer* 589-603
- [25] Merrill T 2000 *Int. J. Heat Mass Transfer* 3287-98
- [26] Hoffmann L and Ziegler F 1999 *ISHPC'99, Proc. Int. Sorption Heat Pump Conf.* 297-300
- [27] Kang Y T, Akisawa A and Kashiwagi T 1999 *Int. J. Refrig.* 250-62
- [28] Kim K J, Berman N S and Wood B D 1996 *Int. J. Refrig.* 322-30
- [29] Miller W A and Perez-Blanco H 1994 *AES-Vol. 31, Proc. Int. Abs. Heat Pump Conf.* 185-202